

Evaluation of computed tomography vascular reconstruction for the localization diagnosis of perigastric mass

Ping Wang, MD^a, Cheng-Zhou Zhang, MD^a, Guang-Bin Wang, MD^b, Yang-Yang Li, MM^c, Xing-Yue Jiang, MD^{a,*}, Fang-Jun Fang, MM^a, Xiao-Xiao Li, MM^a, Jia Bian, MM^a, Xin-Shan Cao, MM^a, Xiao-Fei Zhong, MM^a

Abstract

Background: The aim of this study was to evaluate the utility of computed tomography (CT) vascular reconstruction in the localization diagnosis of perigastric mass.

Methods: Fifty-eight patients with pathologically detected perigastric mass underwent abdominal dynamic contrast-enhanced CT. CT vascular reconstructions were produced from arterial phase data using volume rendering (VR), multiplanar reconstruction (MPR), and maximal intensity projection (MIP). Image analysis was focused on the relationship between the mass, perigastric arteries, and the gastric wall. Localization diagnosis values were compared between CT vascular reconstruction and dynamic-enhanced CT images.

Results: Among the 58 cases of perigastric mass, 41 cases originated from the stomach, 7 cases from the left liver lobe, 6 from the pancreas, 2 from lesser omental bursa, 1 from transverse mesocolon, and 1 from left adrenal gland. The accuracy of CT vascular reconstruction images in the localization diagnosis of perigastric mass was higher than that of dynamic-enhanced CT images (98.3% and 86.2%, respectively, $P = .04$). On the reference level, 35 (35/41) patients with stomach-originated masses showed the mass adjacent perigastric arteries pushed away from the stomach (arterial displacement sign), and 15 (15/17) patients with nonstomach-originated masses showed perigastric arteries between the mass and the stomach (arterial entrapment sign). The sensitivity, specificity, positive predictive value, and negative predictive value of the localization diagnosis of perigastric mass with arterial displacement sign were 85.4%, 100%, 100%, and 73.9%, respectively, and with arterial entrapment sign, 88.2%, 100%, 100%, and 95.3%, respectively.

Conclusion: CT vascular reconstruction can clearly depict the relationship between perigastric mass and adjacent perigastric arteries, which may help us more accurately differentiate between stomach-originated and nonstomach-originated masses compared with original dynamic-enhanced CT images.

Abbreviations: CT = computed tomography, CTA = computed tomography angiography, GISTs = gastrointestinal stromal tumors, MIP = maximum intensity projection, MPR = multiplanar reconstruction, VR = volume rendering.

Keywords: computed tomography, localization diagnosis, mass, multiplanar reconstruction, perigastric artery, vascular reconstruction

Editor: Weisheng Zhang.

PW and CZZ contributed equally to this paper, as the first authors.

This retrospective study was approved by the institutional review board and informed consent was waived.

The authors declare that they have no conflict of interest.

^a Department of Radiology, The Affiliated Hospital of Binzhou Medical University,

^b Shandong Medical Imaging Research Institute, Shandong University,

^c Department of Pathology, The Affiliated Hospital of Binzhou Medical University, Shandong, P. R. China.

* Correspondence: Xing-Yue Jiang, Bin Zhou Medical University, No. 661 Huang-He Second Road, Bin Zhou, Binzhou, Shan Dong 256603, China (e-mail: yswang1013@sina.com).

Copyright © 2018 the Author(s). Published by Wolters Kluwer Health, Inc. This is an open access article distributed under the terms of the Creative Commons Attribution-Non Commercial-No Derivatives License 4.0 (CCBY-NC-ND), where it is permissible to download and share the work provided it is properly cited. The work cannot be changed in any way or used commercially without permission from the journal.

Medicine (2018) 97:26(e11177)

Received: 7 September 2017 / Accepted: 29 May 2018

<http://dx.doi.org/10.1097/MD.0000000000001177>

1. Introduction

Computed tomography (CT) is an imaging examination tool that is widely used to establish medical diagnosis and perform image-guided interventions for gastric cancer. Gastric cancer is the most common tumor of the stomach, with gastric wall thickening being the main CT manifestation.^[1–3] Different types of perigastric mass grow around the stomach; they can be stomach-originated or originate from adjacent organs. Therefore, the corrected localization diagnosis of perigastric mass is very important for further qualitative diagnosis. When the mass is small, CT can usually accurately show the origin of the mass. However, for a larger mass, the adjacent structures are compressed or the boundary between them is ambiguous, which may make it difficult to accurately determine mass origin. Studies utilizing CT angiography (CTA) have clearly depicted perigastric vessels.^[4–8] In this study, we retrospectively reviewed the CT images of 58 patients with perigastric mass and conducted vascular reconstruction in an effort to evaluate the use of CT vascular reconstruction in the localization diagnosis of perigastric mass.

2. Materials and methods

2.1. Patients

We retrospectively reviewed the CT images of 58 patients (33 men and 25 women, mean age 46 ± 12 years, range 21–79 years; the mass size 9.5 ± 8.8 cm, range 2.8–15.9 cm) exhibiting perigastric mass with a proven pathology admitted to our hospital between January 2014 and March 2017. Among the 58 patients, 44 cases were excised through laparotomy, 12 cases were removed by laparoscopy, and 2 cases were confirmed by biopsy. Inclusion criteria were as follows: mass adjacent to the gastric wall, and at least 1 level without fat clearance between the mass and the gastric wall. Exclusion criteria comprised mass with gastric wall thickening or mass located within the outline of the stomach. The appropriate institutional review board approved the study. Informed consent for reviewing the patients' medical records and images was not required.

2.2. CT data acquisition

All examinations were performed by a second-generation dual-source CT scanner (Somatom Definition Flash; Siemens, Erlangen, Germany) in our hospital. Patients with iodine contrast medium allergy were excluded. Tri-phase dynamic contrast-enhanced CT scans were performed in all patients during a single breath hold with patients in the supine position in a single-energy mode. None of the patients were administered an oral contrast agent. An automated power injector (Stellant D; MedRad, Indianola, PA) was used to administer 60 to 80 mL of contrast material (ioversol, 320 g/100 mL) at a rate of 3.5 mL/s followed by 20 mL of saline solution into the antecubital vein via an 18-ga catheter. Tri-phasic contrast-enhanced dynamic exploration during the arterial, portal, and delayed phases was performed separately at 30, 60, and 120 s after contrast material injection. Scan parameters were as follows: tube voltage, 120 kV; detector collimation, 128×0.6 mm; and current flow-dose modulation (CARE Dose4D; Siemens) was enabled with a range of 256 to 436 mAs.

2.3. CT image analysis

CT images were retrospectively evaluated by 2 experienced radiologists (Xing-Yue Jiang, Xin-Shan Cao with 21 and 18 years of experience in abdominal radiology, respectively), who were blinded to the original CT reports and surgical findings on a picture archiving and communication system workstation (Centricity Radiology RA 1000; GE Healthcare, Milwaukee, WI). First, the 2 radiologists performed localization diagnosis of all the masses around stomach using the original contrast enhanced CT images. Second, VR, MPR, and MIP were conducted by the same radiologists using enhanced arterial phase data. They analyzed the relationship between the mass and adjacent vessels, and determined the origin of the mass; consensus was reached. The maximum level of the mass through the mass and stomach contact surface was regarded as the reference level for arterial displacement sign (mass adjacent perigastric arteries were pushed away from the stomach) and arterial entrapment sign (perigastric arteries were shown between the mass and adjacent stomach) (Fig. 1). The perigastric arteries in this article refer to the gastric nutrient arteries close to the wall of the stomach, including the left gastric artery, the right gastric artery, the left gastroepiploic artery, the right gastroepiploic artery, and the short artery of the stomach and its small branch close to the

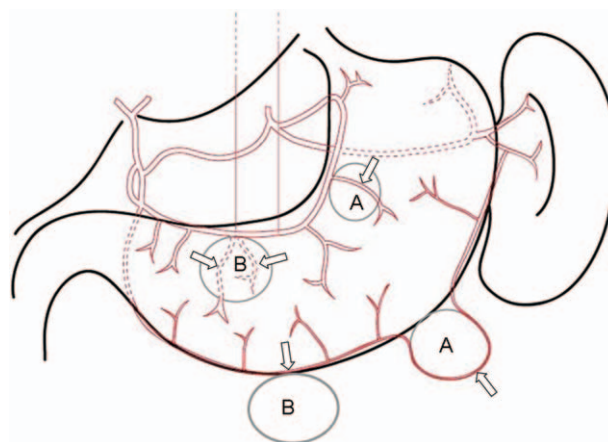


Figure 1. The diagrammatic figures of arterial displacement sign and arterial entrapment sign. (A) Arterial displacement sign (the mass adjacent perigastric arteries were pushed away from the stomach, arrow). (B) Arterial entrapment sign (the perigastric arteries were shown between the mass and the stomach, arrow).

stomach wall. The results of the evaluation were recorded by another resident. The sensitivity, specificity, positive predictive value, and negative predictive value of arterial displacement sign and arterial entrapment sign were calculated accordingly.

2.4. Statistical analysis

Interobserver reliability was assessed by calculating κ coefficients. The κ value can be interpreted as poor ($\kappa = 0$), slight ($\kappa = 0.0-0.2$), fair ($\kappa = 0.21-0.40$), moderate ($\kappa = 0.41-0.60$), substantial ($\kappa = 0.61-0.80$), and almost perfect ($\kappa = 0.81-1.00$).¹⁹ The Chi-square test was used to compare the value of CT vascular reconstruction and original contrast-enhanced CT images for the localization diagnosis of perigastric mass. P values $< .05$ were statistically significant. Statistical analysis was performed with SPSS (v. 22.0; IBM, Armonk, NY).

3. Results

3.1. Types and origins of perigastric mass

Among the 58 patients, 41 masses originated from the gastric serosa (28 gastric stromal tumors, 7 schwannomas, 4 leiomyoma, and 2 lipoma), 22 originated from the body, 13 originated from the gastric fundus and cardia region, and 6 originated from the antrum. The remaining 17 patients had nonstomach-originated masses; 7 cases originated from the left liver lobe (3 hepatocellular carcinoma, 3 metastatic tumor, 1 inflammatory myofibroblastic tumor), 6 cases from the pancreas (3 cystadenoma, 2 solid pseudopapillary neoplasm, and 1 cystadenocarcinoma), 2 lesser omental cysts, 1 transverse mesocolon hemangioma, and 1 adrenal nonfunctional adenoma (Table 1).

3.2. Evaluation of CT vascular reconstruction for the localization diagnosis of perigastric mass

The interobserver reliability of the radiologists to determine the origin of all the masses around stomach was almost perfect using the original contrast enhanced CT images ($\kappa = 0.865$), and using CT vascular reconstruction ($\kappa = 0.930$).

Table 1
Cases of perigastric mass.

Origin of the mass	Pathologic diagnosis	number	Number of misdiagnosis		χ^2	P
			Original enhanced CT images	Combined CT vascular reconstruction		
Gastric	Gastrointestinal stromal tumors	28	4	1	4.336*	.04
	Schwannomas	7	0	0		
	Leiomyoma	4	0	0		
	Lipoma	2	0	0		
Liver	Liver cancer	3	0	0		
	Metastatic tumor	3	2	0		
	Inflammatory myofibroblastic tumor	1	1	0		
Pancreas	Cystadenoma	3	0	0		
	Solid pseudopapillary tumor	2	0	0		
	Cystadenocarcinoma	1	0	0		
Lesser omental	Cyst	2	0	0		
Mesocolon transversum	Hemangiomas	1	1	0		
Adrenal	Nonfunctional adenoma	1	0	0		

* Continuity correction.

The accuracy of original contrast-enhanced CT images in the localization diagnosis of perigastric mass was 86.2% (50/58), with misdiagnosis in eight cases. The accuracy of CT vascular reconstruction images was 98.3% (57/58), with misdiagnosis in 1 case (Table 1). The localization diagnosis accuracy of CT vascular reconstruction was significantly higher than that of the original contrast-enhanced CT images ($P = .04$).

The cases of arterial displacement sign and arterial entrapment sign detected on the reference level are presented in Tables 2 and 3, respectively. In all 41 patients with stomach-originated masses, no perigastric arteries were visualized between the mass and the stomach on the reference level, and 35 (35/41) patients showed the adjacent perigastric arteries pushed away from the stomach (Fig. 2). In 15 (15/17) patients with nonstomach-originated masses, perigastric arteries occurred between the mass and the stomach on the reference level, and no perigastric arteries were pushed away from the stomach in all 17 patients (Figs. 3–5). The sensitivity, specificity, positive predictive value, and negative predictive value of the localization diagnosis of perigastric mass with arterial displacement sign were 85.4%, 100%, 100%, and 73.9%, respectively, and with arterial entrapment sign, 88.2%, 100%, 100%, and 95.3%, respectively (Table 4).

In 2 gastrointestinal stromal tumors (GISTs), the blood supply was from the adjacent gastric artery (Fig. 6), and in 2 left liver lobe masses, it was from the left hepatic artery (Fig. 7).

4. Discussion

In this study, we investigated the value of CT vascular reconstruction in the localization diagnosis of perigastric mass.

Table 2
Cases of arterial displacement sign detected on the reference level.

Arterial displacement sign	Pathological results		Total
	Positive (stomach-originated)	Negative (nonstomach-originated)	
Positive	35	0	35
Negative	6	17	23
Total	41	17	58

For patients with known or suspected gastric tumors, CT is the mainstay for preoperative staging and postoperative follow-up, in addition to gastroscopy.^[3,10] The recent development of dual-source CT (single or dual-source mode) has led to significant improvements in spatial resolution and scanning speed, which can eliminate the change in blood vessel position caused by gastric peristalsis.^[11] High spatial resolution is needed to visualize small vessels, and fast scanning speed is desirable for the evaluation of arteries with no overlying veins.^[12] To date, many studies on the clinical application of CT in the stomach have been performed, mainly for gastric tumors.^[13–15] However, some perigastric masses arise in the submucosa, muscularis propria, or serosa of the gastric wall, or originate from organs adjacent to the stomach. Large masses and unclear boundaries between the mass and stomach may make accurate localization diagnosis before surgery difficult. A few studies have demonstrated the value of CTA in the simulation perigastric vascular anatomy.^[4–8] To the best of our knowledge, there has been no study to date on the localization diagnosis value of CT vascular reconstruction for perigastric mass. In this study, the celiac trunk and its branches were reconstructed from arterial phase data, and the relationship between the mass, perigastric artery, and gastric wall were clearly demonstrated.

Gastric submucosal tumors mainly include GISTs, schwannomas, leiomyomas, and lymphoma. GIST is the most common submucosal tumor of the stomach^[16]; a gastric stromal tumor predominance was also observed in our study (28/41 patients). Most large perigastric masses as potential malignant tumors require surgical resection. Laparoscopic surgery has significantly advanced gastrointestinal surgery because it is considered to be

Table 3
Cases of arterial entrapment sign detected on the reference level.

Arterial entrapment sign	Pathological results		Total
	Positive (nonstomach-originated)	Negative (stomach-originated)	
Positive	15	0	15
Negative	2	41	43
Total	17	41	58

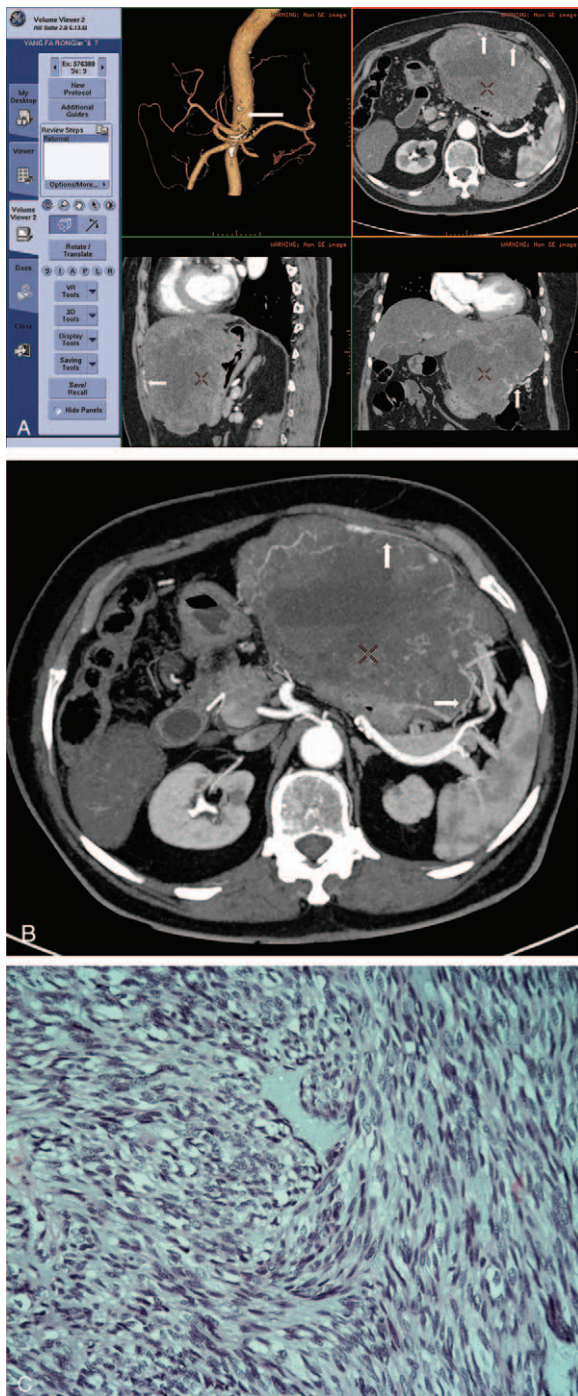


Figure 2. A 73-year-old woman with a gastric stromal tumor. (A) Vascular reconstruction shows the celiac axis, common hepatic artery, left gastric artery, and the splenic artery and their branches. Note that the left gastric artery originates from the celiac trunk (long arrow) and the left gastroepiploic arteries are pushed away from the stomach (arterial displacement sign, short arrow). (B) Multiplanar reconstruction image showing arterial displacement sign (short arrow). (C) Histologically, the tumor mainly consists of spindle cells, arranged in a braid shape, with abnormal cells, and mucoid degeneration in some areas.

minimally invasive and improves the quality of life for patients after surgery, especially for small tumors.^[5] However, laparoscopic surgery is technically challenging derived from the limited visibility of surgical fields. Therefore, knowledge of detailed local anatomy is essential for laparoscopic surgery. Due to the high spatial resolution, CT vascular reconstruction images derived

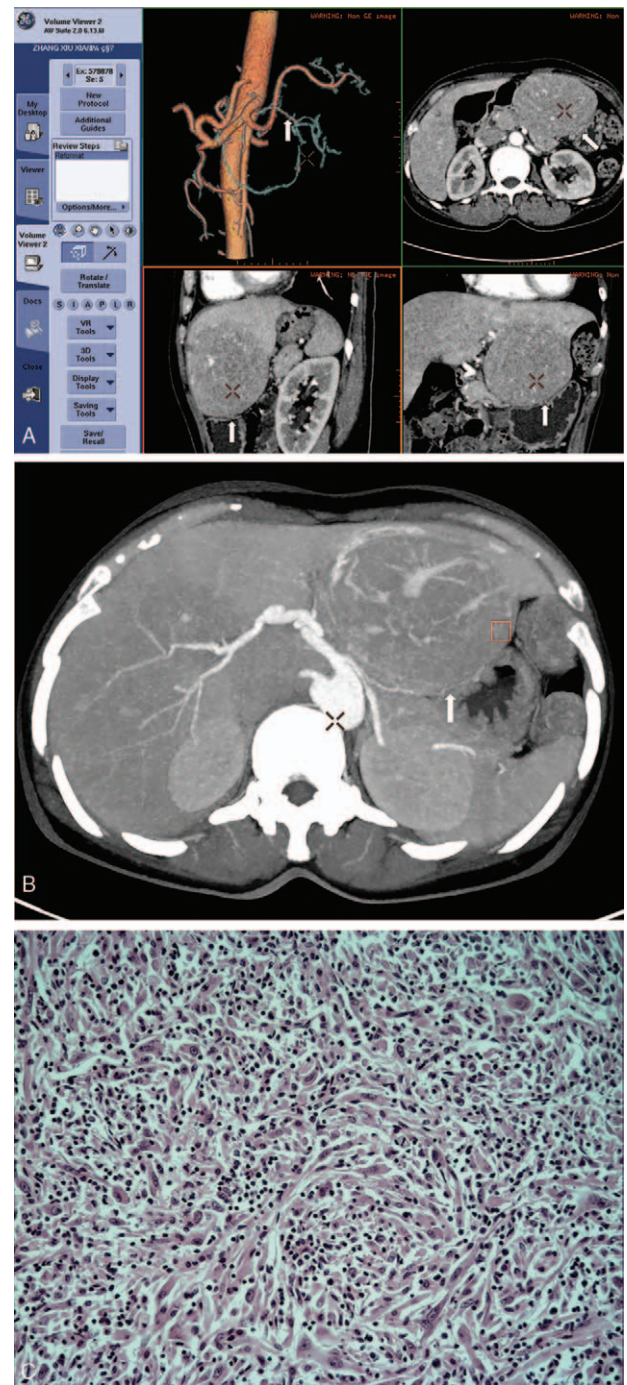
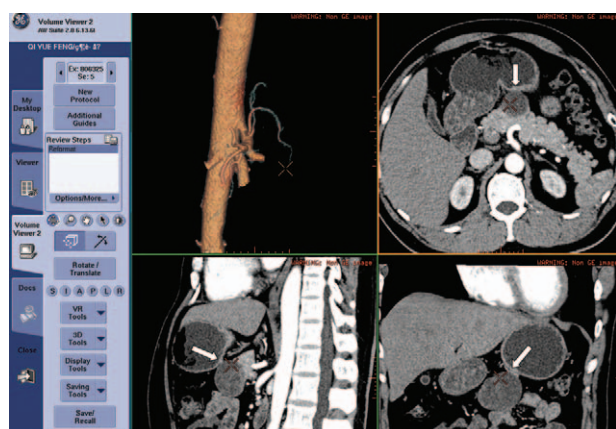


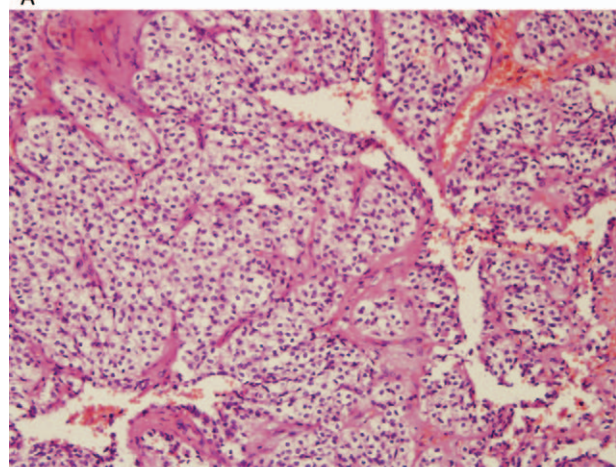
Figure 3. A 47-year-old woman with an inflammatory myofibroblastic tumor of the left liver lobe. (A) and (B) The left gastric artery is shown between the mass and the stomach (arterial entrapment sign, arrow). (C) Histologically, the tumor mainly consists of spindle cells, arranged in whirlpool-like shape, and considerable chronic inflammatory cell infiltration can be seen in the stroma.

from original contrast-enhanced CT can clearly show vascular structures and soft tissue anatomy.^[4]

Our results showed that the accuracy of CT vascular reconstruction images in the localization diagnosis of perigastric mass is higher than that of original dynamic contrast-enhanced CT images. Original dynamic contrast-enhanced CT misdiagnosed 8 cases, there may be several reasons for this. First, the boundary of 2 gastric stromal tumors originating from the lesser

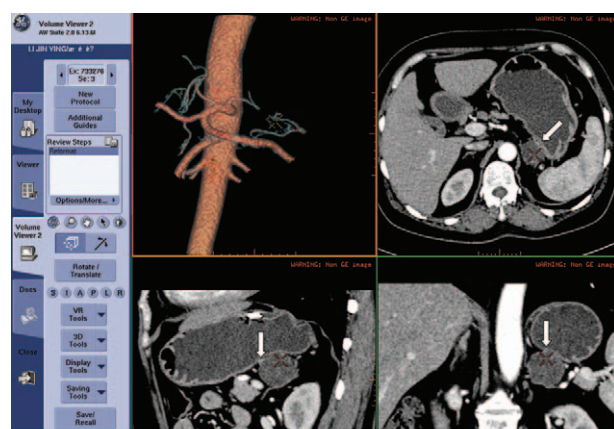


A

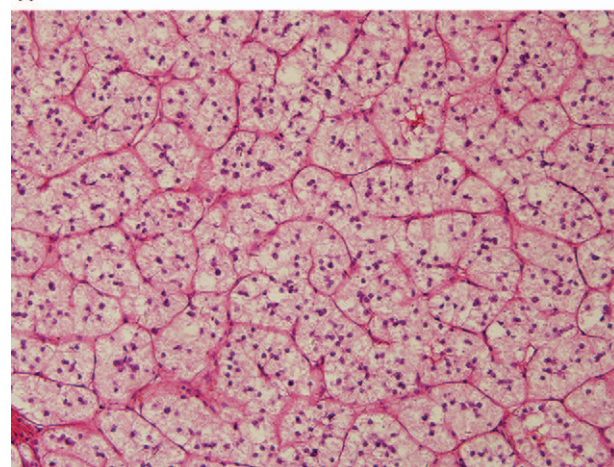


B

Figure 4. A 36-year-old woman with a solid pseudopapillary neoplasm of the pancreas. (A) The left gastric artery is shown between the mass and the stomach (arterial entrapment sign, arrow). (B) Histologically, the size of the tumor cells is uniform with a solid flake, with different degrees of sclerosis, and some part of the region is disintegrated to form a pseudopapillary structure.



A



B

Figure 5. A 58-year-old man with an adenoma of the left adrenal gland. (A) The short artery of stomach is shown between the mass and the stomach (arterial entrapment sign, arrow). (B) Histologically, the tumor cells show acinar arrangement, and the cytoplasm of the cell is bright and rich.

curvature was not clear from the adjacent hepatic left lobe, which led to a misdiagnosis of left liver lobe tumor. The volumes of another 2 cases of gastric stromal tumor were large, the main parts of the tumors were located below the stomach, the gastric morphology changed slightly, and the boundaries of the tumors were unclear from the adjacent pancreas. This therefore led to a misdiagnosis of pancreatic tumor. Second, an inflammatory myofibroblastic tumor and 2 metastatic tumors of the left liver lobe had large volumes, were hypervascular, and grew outside of the liver outline. The boundary between the tumor and adjacent gastric wall of the lesser curvature was unclear leading to a misdiagnosis of gastric stromal tumors, the most common

mesenchymal tumor of the stomach.^[17,18] Third, in 1 case, the mass originated from transverse mesocolon hemangioma. In this case, multilocular cystic change occurred and the enhancement of the tumor was not obvious, which was not consistent with the enhancement of typical hemangioma,^[19] and the tumor was misdiagnosed as gastric tumor due to lack of understanding of the disease (Fig. 8).

On the reference level with MPR, we found that perigastric arteries adjacent to the masses were pushed away from the stomach in 85.4% (35/41) of stomach-originated masses, and no perigastric arteries or their tributaries were visualized between the masses and the stomach. We also found arterial entrapment

Table 4

Evaluation of arterial displacement/entrapment sign of localization diagnosing perigastric mass.

	Sensitivity (%)	Specificity (%)	Positive predictive value (%)	Negative predictive value (%)
Arterial displacement sign	85.4	100	100	73.9
Arterial entrapment sign	88.2	100	100	95.3

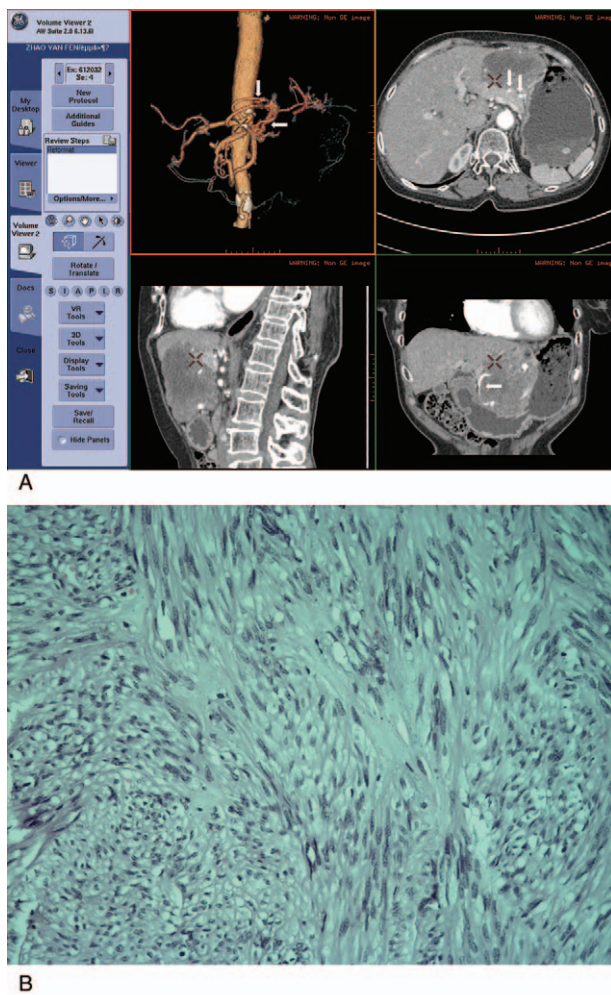


Figure 6. A 58-year-old man with a gastric stromal tumor. (A, vascular reconstruction and multiplanar reconstruction) show that the blood supply is from the thickened left gastric artery (arrow). (B) Histologically, the tumor mainly consists of macrospindle cells arranged in a braid shape, without abnormal cells.

sign in 88.2% (15/17) of nonstomach-originated masses, but no arterial displacement sign. The high positive predictive value and specificity of arterial displacement sign indicated an accurate localization diagnosis of stomach-originated masses, while arterial entrapment sign indicated an accurate localization diagnosis of nonstomach-originated masses. We observed 6 stomach-originated masses without arterial displacement sign and 2 nonstomach-originated masses without arterial entrapment sign. We believe that this may be associated with the tenuous lumens of the perigastric arteries adjacent to the mass, which are not easily demonstrated by tumor compression. On the contrary, CT reconstruction images can be used to observe the relationship between the tumor and adjacent vessels from any viewpoint, which is helpful for the establishment of a surgical plan and ensures safety.^[7]

Our study has some limitations. First, our study was performed retrospectively, and there are no images of extragastric mass with gastric wall invasion in our patients; we suspect that if there is an invasion of the gastric wall, and it may be difficult to demonstrate arterial entrapment sign. Second, the number of cases and

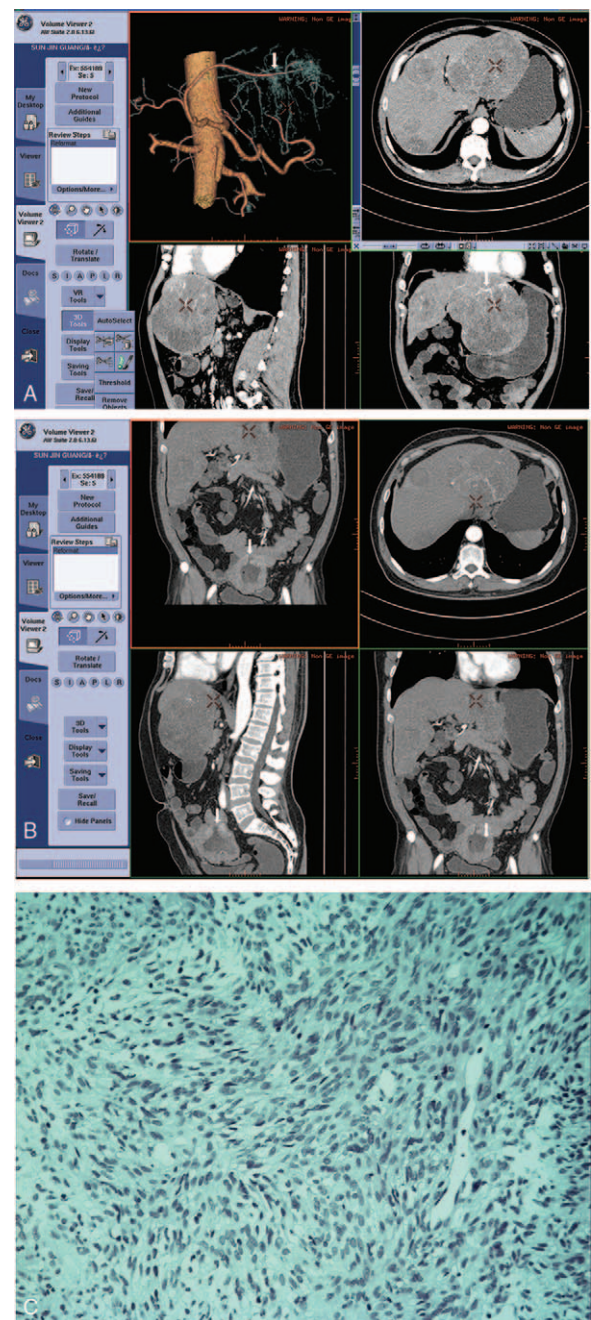


Figure 7. A 48-year-old man with a metastatic tumor. (A) Multiple tumors in the liver are shown, and the vascular reconstruction image shows that the blood supply is from the left hepatic artery (arrow). (B) The primary tumor is a small intestinal stromal tumor (arrow). (C) Histologically, the tumor mainly consists of spindle cells arranged in bundles and in a braid shape.

diseases was relatively small, although our study included a larger number of patients than previous studies. Finally, we did not discuss additional tumor localization signs not originating from the stomach. Moreover, the arterial displacement sign and arterial entrapment sign will just add confidence of differentiating nongastric with gastric origin of mass, hence mention about contrast enhancement pattern (wash in and wash out) of the mass and fat planes with stomach and adjacent structure still remain the chief diagnostic clues.

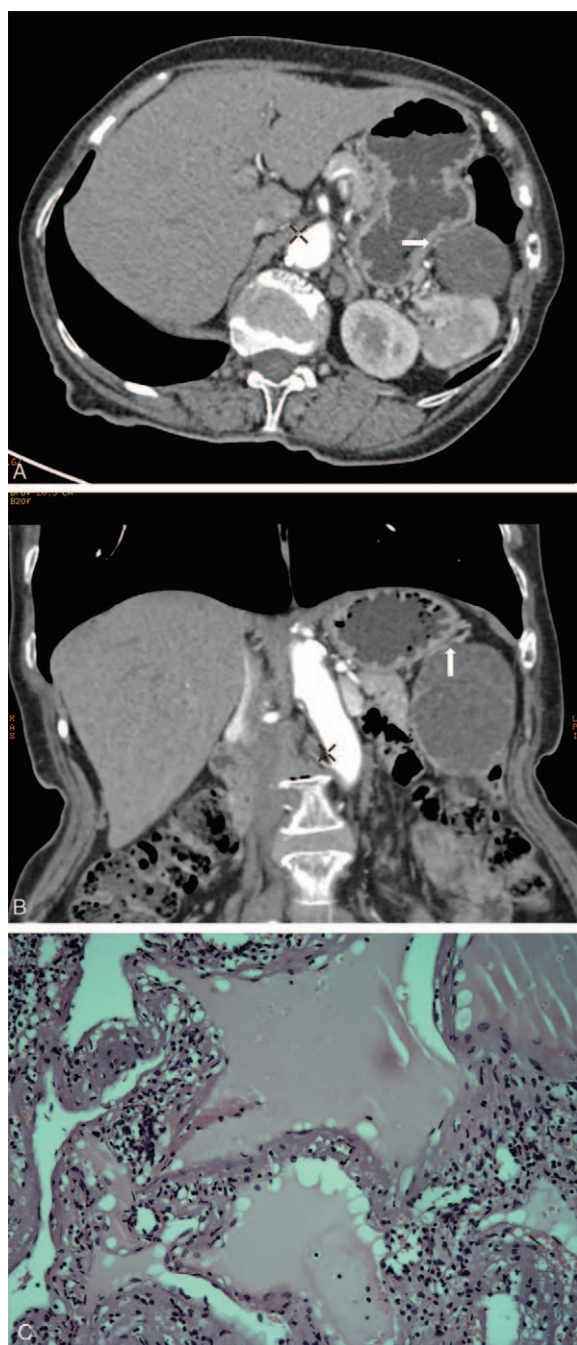


Figure 8. A 71-year-old woman with a transverse mesocolon hemangioma. (A and B) The left gastroepiploic arteries are shown between the mass and the stomach (arrow). © Histologically, the tumor mainly consists of dilated lymphatics and blood vessels, the lumen size differs, and the tube wall is irregular.

5. Conclusion

CT arterial vascular reconstruction images can accurately determine the origin of perigastric mass, in particular the determination of whether the mass originated from the stomach, which has great significance for further qualitative diagnosis. In addition, vascular reconstruction can determine the exact relationship between the peripheral tumor and adjacent vessels,

organs, or tissues, which is helpful for the establishment of a surgical plan and ensures safety.

Author contributions

Ping Wang and Cheng-Zhou Zhang contributed equally to this work, as the first authors. Study concept and design: Cheng-Zhou Zhang, Ping Wang, Guang-Bin Wang, and Xing-Yue Jiang; acquisition of data: Ping Wang, Fang-Jun Fang, Xiao-Xiao Li, Xiao-Fei Zhong, and Jia Bian; analysis and interpretation of data: Cheng-Zhou Zhang, Xing-Yue Jiang, Xin-Shan Cao, and Chuan-Ting Li; drafting of the manuscript: Ping Wang; critical revision of the manuscript for important intellectual content: Cheng-Zhou Zhang, Ping Wang, and Xing-Yue Jiang.

Data curation: Junfang Fang, Jia Bian.

Formal analysis: Xiaoxiao Li.

Methodology: Guangbin Wang, Xing Yue Jiang, Xinshan Cao, Xiaofei Zhong.

Project administration: Xing Yue Jiang.

Resources: Yangyang Li.

Writing – original draft: Ping Wang, Chengzhou Zhang.

Writing – review & editing: Xing Yue Jiang.

References

- [1] Tan CH, Peungjesada S, Charnsangavej C, et al. Gastric cancer: patterns of disease spread via the perigastric ligaments shown by CT. *AJR Am J Roentgenol* 2010;195:398–404.
- [2] Johnson PT, Horton KM, Fishman EK. Hypervascular gastric masses: CT findings and clinical correlates. *AJR Am J Roentgenol* 2010;195: W415–20.
- [3] Vukobrat-Bijedic Z, Husic-Selimovic A, Sofic A, et al. Comparability of diagnostic methods: proximal endoscopy, CT and EUS in determining stomach tumor localization and their importance in the preoperative analysis of process progression. *Acta Inform Med* 2013;21:246–9.
- [4] Lee SW, Shinohara H, Matsuki M, et al. Preoperative simulation of vascular anatomy by three-dimensional computed tomography imaging in laparoscopic gastric cancer surgery. *J Am Coll Surg* 2003;197:927–36.
- [5] Osaki T, Saito H, Murakami Y, et al. Usefulness of preoperative assessment of perigastric vascular anatomy by dynamic computed tomography for laparoscopic gastrectomy. *Yonago Acta Med* 2015; 58:157–64.
- [6] Wu Y, Chen G, Wu P, et al. CT imaging-based determination and classification of anatomic variations of left gastric vein. *Surg Radiol Anat* 2017;39:249–55.
- [7] Natsume T, Shuto K, Yanagawa N, et al. The classification of anatomic variations in the perigastric vessels by dual-phase CT to reduce intraoperative bleeding during laparoscopic gastrectomy. *Surg Endosc* 2011;25:1420–4.
- [8] Kumano S, Tsuda T, Tanaka H, et al. Preoperative evaluation of perigastric vascular anatomy by 3-dimensional computed tomographic angiography using 16-channel multidetector-row computed tomography for laparoscopic gastrectomy in patients with early gastric cancer. *J Comput Assist Tomogr* 2007;31:93–7.
- [9] Landis JR, Koch GG. The measurement of observer agreement for categorical data. *Biometrics* 1977;33:159–74.
- [10] Chai Y, Xing J, Gao J, et al. Feasibility of virtual nonenhanced images derived from single-sourcefast kVp-switching dual-energy CT in evaluating gastric tumors. *Eur J Radiol* 2016;85:366–72.
- [11] Miyaki A, Imamura K, Kobayashi R, et al. Preoperative assessment of perigastric vascular anatomy by multidetector computed tomography angiogram for laparoscopy-assisted gastrectomy. *Langenbecks Arch Surg* 2012;397:945–50.
- [12] Abdel Razek AA, Denewer AT, Hegazy MA, et al. Role of computed tomography angiography in the diagnosis of vascular stenosis in head and neck microvascular free flap reconstruction. *Int J Oral Maxillofac Surg* 2014;43:811–5.
- [13] Yao J, Yang ZG, Chen HJ, et al. Gastric adenocarcinoma: can perfusion CT help to noninvasively evaluate tumor angiogenesis? *Abdom Imaging* 2011;36:15–21. doi: 10.1007/s00261-010-9609-5.

- [14] Hyung WJ, Kim YS, Lim JS, et al. Preoperative imaging of sentinel lymph nodes in gastric cancer using CT lymphography. *Yonsei Med J* 2010;51:407–13.
- [15] Matoba M, Oota K, Toyoda I, et al. Usefulness of 4D-CT for radiation treatment planning of gastric MZBCL/MALT. *J Radiat Res* 2012;53:333–7.
- [16] Choi JW, Choi D, Kim KM, et al. Small submucosal tumors of the stomach: differentiation of gastric schwannoma from gastrointestinal stromal tumor with CT. *Korean J Radiol* 2012;13:425–33.
- [17] O'Neill AC, Shinagare AB, Kurra V, et al. Assessment of metastatic risk of gastric GIST based on treatment-naive CT features. *Eur J Surg Oncol* 2016;42:1222–8.
- [18] Chong A, Ha JM, Hong R, et al. Inflammatory myofibroblastic tumor mimicking gastric gastrointestinal stromal tumor on 18F-FDG PET/CT. *Clin Nucl Med* 2014;39:725–7.
- [19] Tian C, Zheng Y, Ren X, et al. A giant abdominal cystic tumour: mesentery cystic lymphangioma. *Dig Liver Dis* 2015;47:816–7.